Understanding the surface structure of catalysts and 2D materials at the atomic scale

Boden, D.

Chapter 7

Summary & Outlook

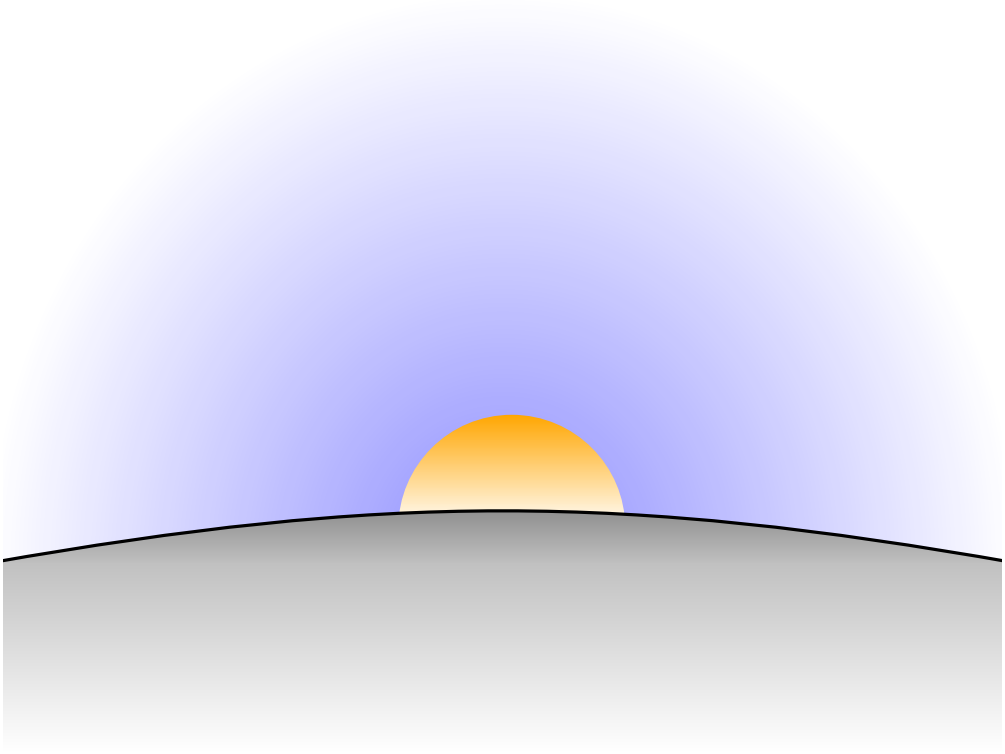

The work in this thesis demonstrates how to obtain an atomic-scale picture of a diverse set of complex surface structures observed using STM, under disparate conditions. Chapters 4−6 each represent a different approach to answer the same question: How can we find out what a surface looks like at the atomic scale? By employing appropriate theoretical tools that complement the experimental conditions and measurement techniques, it is possible to compare the results from theory and experiment in an intuitive manner to obtain additional insights. Additionally, Chapter 4 shows that theoretical studies, which do not take experimental conditions into account appropriately, can lead to wrong conclusions.

It is very tempting to model 2D materials computationally as free-standing sheets in vacuum, since this vastly decreases the complexity and computational cost of (electronic) structure calculations. This approach is often justified by presumed weak interactions between substrate and the 2D materials. However, the best-quality 2D materials are most often manufactured directly on a substrate, and not by exfoliation of the bulk material, which means that interactions with the substrate actually play an important role in practice. In Chapter 4 we show how we can grow sheets of single-layer cobalt sulfide with a structure analogous to other transition metal dichalcogenides (TMDCs), such as TiS_2 and MoS_2. These experimental findings are in contrast to previous DFT studies on free-standing TMDCs, which predict that Co and S are not able to form a stable 2D TMDC. CoS_2 is remarkable, because no bulk crystal structures consisting of layered S-Co-S sheets exist, unlike TiS_2 and most other known TMDCs. In order to resolve this apparent discrepancy between theory and experiment, DFT calculations in Chapter 4 include not only the CoS_2 sheet, but also the Au(111) substrate explicitly. This way, we find excellent agreement between theory and experiments, since DFT shows that the formation of this novel 2D TMDC is facilitated by the strong interaction between gold and sulfur. From the electronic structure obtained from DFT and STM, we also determine that, unlike most 2D TMDCs, 2D CoS_2 is metallic, which opens up possibilities for novel applications.

Since the gold substrate seems to aid the formation of 2D cobalt sulfide, it is conceivable that gold might also facilitate the formation of other novel 2D transition metal disulfides. The CoS_2 sheets were manufactured by exposing Co nanoparticles on Au(111) to H_2S at high temperatures, a recipe which can be readily repeated using (a combination of) other transition metals, to create other novel 2D TMDCs. Additionally, when the cobalt sulfide in Chapter 4 is cooled down in UHV instead of H_2S, the surface of the sheets appears as flower-like rings in STM images, which are reminiscent of buckled silicene on Ag(111), as illustrated in Figure 7.1.[1–5] This pattern is likely a reconstruction resulting from a sulfur deficiency in the top layer, as similar reconstructions have been observed with STM on other 2D TMDCs that are grown non-stoichiometrically, or have been (intentionally) damaged.[6,7] Since similar reconstructions seem to occur in many 2D TMDCs, a comprehensive investigation into the reconstruction of chalcogenide-deficient 2D TMDCs and their unique properties would be compelling. Naturally, to investigate other (defected) 2D TMDCs theoretically, the gold substrate should be included explicitly in electronic structure calculations.

In situ STM experiments on the initial oxidation of Pt(111) by van Spronsen et al.[8] found complex intermediary platinum surface oxides, consisting of spoke-wheel and stripe structures. While the stripes have been investigated extensively,[9] the spoke

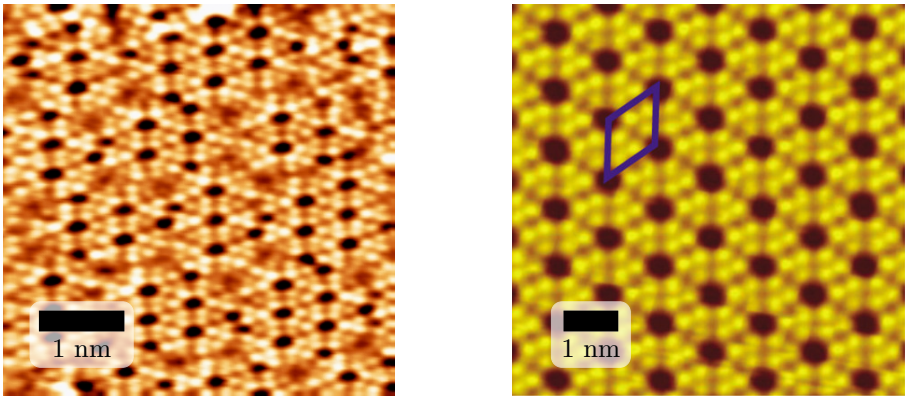

Figure 7.1: **Left:** STM image of sulfur-deficient 2D cobalt sulfide sheets on Au(111), obtained by M.K. Prabhu. $I_{tunnel} \approx 100$ pA and $V_{bias} = -1$ V. **Right:** STM image of buckled silicene on Ag(111). The 1.18 × 1.18 nm^2 surface unit cell is indicated in purple. The image was obtained with a -1 V bias on the STM tip. Adapted from Feng et al.[1] *Copyright 2012 American Chemical Society.*

wheels were poorly understood, owing to their size and complexity. The scale of the spoke wheels, as observed with STM, is too large for DFT. In addition, obtaining a reasonable initial guess for a structure this size is problematic, especially since there is no available experimental data on the stoichiometry or oxidation states of the platinum and oxygen on the surface. In Chapter 5, atomistic thermodynamics is employed based on an established reactive force field to investigate the structure and stability of spoke wheels at the elevated temperature (>530 K) and pressure (1–4 bar) conditions of the *in situ* experiments. At those conditions, the thermodynamic stability of the structural model for the spoke wheel is similar to that of the stripes, while the degree of surface oxidation is much lower. The spoke-wheel structure is found to be much more stable than partially formed stripes with a similar degree of oxidation. These results are consistent with experimental findings, where the spoke wheel is observed first, at slightly lower oxygen pressures.

The results presented in Chapter 5 suggest that the spoke wheels are likely not thermodynamically more stable than the PtO_2 stripes, even at the experiment conditions at which they were observed. Still, it would be valuable to obtain a more accurate estimate for the vibrational free energy, to improve the accuracy of the atomistic thermodynamics approach. Since DFT calculations on the spoke-wheel structure obtained in Chapter 5 are not feasible, it is challenging to obtain accurate information on the vibrational modes needed to calculate the vibrational free energy of the spoke wheels explicitly. Although such calculations are currently beyond reach for the spoke wheels, they might become tractable in the future. The development of linear scaling techniques for DFT, suitable for metallic systems, could enable electronic structure calculations directly.[10–13] Alternatively, further refinement of the pre-existing Pt-O parametrization, or the development of novel parametrizations based on machine-learning techniques wich can account for long-range (electrostatic) interactions may

allow for vibrational free energy calculations without the need for explicit electronic structure calculations.[14–16]

Although the slow speed of the initial oxidation of Pt(111) allows for a reasonable description of the observed surface structures by assuming a quasi-equilibrium, a comprehensive understanding of this surface under oxidative conditions requires a description of the kinetics of the oxidation process. In fact, recent work shows how high kinetic diffusion barriers strongly influence the formation and structure of surface oxides on Pt(111) under electrochemical conditions.[17] As indicated in Section 5.4, adaptive kinetic Monte Carlo simulations and further molecular dynamics simulations, at a scale that allows the spoke wheels to form, would be an important step forward.[18–21]

The effect of reactants on the catalyst surface at pressures beyond UHV is demonstrated in Chapter 6. Unlike what is observed with STM under UHV conditions, the Rh(100) surface is drastically changed when exposed to atmospheric pressures of CO. *In situ* STM results indicate the formation of rhodium islands on the (100) terraces, in conjunction with roughening of the step edges. Interestingly, roughening does not occur at the same pressures of NO, even though the Rh-NO bond is found to be much stronger than the Rh-CO bond. In fact, compared to dosing only CO at atmospheric pressure, a decrease in surface roughening is observed when co-dosing NO and CO, even at identical CO partial pressures. This is remarkable, since NO is reported to promote Rh-carbonyl formation on nanoparticles by weakening Rh-Rh bonds of rhodium surface atoms, which promotes catalyst disintegration.[22–25] The adsorption of NO and CO on the Rh(100) surface, at the experimental conditions, is investigated using atomistic thermodynamics based on DFT calculations and supported by LEED and AES results. The results from atomistic thermodynamics show that NO likely inhibits CO adsorption by blocking the CO adsorption sites, thereby preventing carbonyl formation and decreasing surface roughening.

At room temperature, the DFT-based phase diagram for NO and CO adsorption on Rh(100) can apparently be accurately described using atomistic thermodynamics, however, it would be interesting to assess the accuracy of this approach at reaction conditions (>520 K).[26–29] Observing adsorbed species on the surface at room temperature directly using *in situ* STM may prove challenging, however, obtaining definitive and quantitative information on the adsorbates present on the surface using complementary *in situ* techniques, such as NAP-XPS or PM-RAIRS, would be a pertinent goal in the future.

References

(1) Feng, B.; Ding, Z.; Meng, S.; Yao, Y.; He, X.; Cheng, P.; Chen, L.; Wu, K. *Nano Letters* **2012**, *12*, 3507–3511.

(2) Vogt, P.; De Padova, P.; Quaresima, C.; Avila, J.; Frantzeskakis, E.; Asensio, M. C.; Resta, A.; Ealet, B.; Le Lay, G. *Physical Review Letters* **2012**, *108*, 155501.

(3) Lin, C.-L.; Arafune, R.; Kawahara, K.; Tsukahara, N.; Minamitani, E.; Kim, Y.; Takagi, N.; Kawai, M. *Applied Physics Express* **2012**, *5*, 045802.

(4) Majzik, Z.; Tchalala, M. R.; Svec, M.; Hapala, P.; Enriquez, H.; Kara, A.; Mayne, A. J.; Dujardin, G.; Jelínek, P.; Oughaddou, H. *Journal of Physics: Condensed Matter* **2013**, *25*, 225301.

(5) Liu, Z.-L.; Wang, M.-X.; Xu, J.-P.; Ge, J.-F.; Le Lay, G.; Vogt, P.; Qian, D.; Gao, C.-L.; Liu, C.; Jia, J.-F. *New Journal of Physics* **2014**, *16*, 075006.

(6) Komsa, H.-P.; Krasheninnikov, A. V. *Advanced Electronic Materials* **2017**, *3*, 1600468.

(7) Lehtinen, O. et al. *ACS Nano* **2015**, *9*, 3274–3283.

(8) Van Spronsen, M. A.; Frenken, J. W. M.; Groot, I. M. N. *Nature Communications* **2017**, *8*, 429.

(9) Hanselman, S.; McCrum, I. T.; Rost, M. J.; Koper, M. T. M. *Physical Chemistry Chemical Physics* **2020**, *22*, 10634–10640.

(10) Nakata, A.; Bowler, D. R.; Miyazaki, T. *arXiv preprint arXiv:2204.12894* **2022**.

(11) Bowler, D.; Miyazaki, T.; Gillan, M. *Journal of Physics: Condensed Matter* **2002**, *14*, 2781.

(12) Skylaris, C.-K.; Haynes, P. D.; Mostofi, A. A.; Payne, M. C. *Journal of Physics: Condensed Matter* **2008**, *20*, 064209.

(13) Tong, L. Metal Conquest, 2011.

(14) Chen, C.; Deng, Z.; Tran, R.; Tang, H.; Chu, I.-H.; Ong, S. P. *Physical Review Materials* **2017**, *1*, 043603.

(15) Botu, V.; Chapman, J.; Ramprasad, R. *Computational Materials Science* **2017**, *129*, 332–335.

(16) Behler, J.; Csányi, G. *The European Physical Journal B* **2021**, *94*, 1–11.

(17) Mascaró, F. V.; McCrum, I. T.; Koper, M. T.; Rost, M. J. *Journal of The Electrochemical Society* **2022**, *169*, 112506.

(18) Henkelman, G.; Jónsson, H. *The Journal of Chemical Physics* **2001**, *115*, 9657–9666.

(19) Fantauzzi, D.; Krick-Calderón, S.; Mueller, J. E.; Grabau, M.; Papp, C.; Steinrück, H.-P.; Senftle, T. P.; van Duin, A. C. T.; Jacob, T. *Angewandte Chemie International Edition* **2017**, *56*, 2594–2598.

(20) Jung, C. K.; Braunwarth, L.; Jacob, T. *Journal of Chemical Theory and Computation* **2019**, *15*, 5810–5816.

(21) Fantauzzi, D.; Bandlow, J.; Sabo, L.; Mueller, J. E.; van Duin, A. C. T.; Jacob, T. *Physical Chemistry Chemical Physics* **2014**, *16*, 23118–23133.

(22) Yates, J. T.; Kolasinski, K. *The Journal of Chemical Physics* **1983**, *79*, 1026–1030.

(23) McKee, M. L.; Worley, S. D. *The Journal of Physical Chemistry* **1988**, *92*, 3699–3700.

(24) Novák, E.; Sprinceana, D.; Solymosi, F. *Applied Catalysis A: General* **1997**, *149*, 89–101.

(25) Bergeret, G.; Gallezot, P.; Gelin, P.; Taarit, Y. B.; Lefebvre, F.; Naccache, C.; Shannon, R. D. *Journal of Catalysis* **1987**, *104*, 279–287.

(26) Herman, G.; Peden, C.; Schmieg, S.; Belton, D. *Catalysis Letters* **1999**, *62*, 131–138.

(27) Berlowitz, P. J.; Oh, S. H.; Goodman, D. W.; Fisher, G. B.; Blair, D. S.; Peden, C. H. F. *The Journal of Physical Chemistry* **2005**, *92*, 1563–1567.

(28) Jansen, M. M.; Caniaz, O.; Nieuwenhuys, B. E.; Niemantsverdriet, J. W. *Langmuir* **2010**, *26*, 16239–16245.

(29) Exner, K. S.; Over, H. *Accounts of Chemical Research* **2017**, *50*, 1240–1247.